Desalination and Water Treatment
www.deswater.com
doi: 10.1080/19443994.2013.827307

52 (2014) 626–632
January

Taylor & Francis
Taylor & Francis Group

Development of nanofiltration membrane separation prediction system for binary salt solutions

Nora'aini Ali[a,*], Norhaslina Mohd Sidek[b], Ilyani Abdullah[c]

[a]*Faculty of Science & Technology, Department of Engineering Science, Universiti Malaysia Terengganu, Kuala Terengganu, Terengganu 21030, Malaysia*
Email: noraaini@umt.edu.my
[b]*Faculty of Chemical Engineering, Universiti Teknologi MARA (Terengganu), Dungun Campus, Dungun, Terengganu 23000, Malaysia*
[c]*Faculty of Science & Technology, Department of Mathematics, Universiti Malaysia Terengganu, Kuala Terengganu, Terengganu 21030, Malaysia*

Received 9 March 2013; Accepted 30 March 2013

ABSTRACT

The previous studies on nanofiltration (NF) mainly focused on the work to update the existing predictive models to enhance its application in order to optimize the separation prediction. There is still lack of research which successfully creates a user-friendly system for separation process prediction optimization. In this study, a MATLAB®-based NF prediction system (NF-BIN) utilizing Donnan Steric Pore model with application of m-file programming and graphical user interface was developed specifically for binary salt solutions treatment. Prior to the prediction, locally fabricated polyethersulfone membranes with three different polymer concentrations, 19, 21, and 23%, were characterized in terms of pore radius, r_p ratio of membrane thickness to porosity, $\Delta x/A_k$ and effective charge density, X_d using uncharged, and charged solutes rejection data. Further the rejection prediction performance was carried out to predict the percentage contribution of ion transport mechanism of three transport modes: diffusion, electromigration, and convection as described in Extended Nernst–Planck equation. The results obtained from this study indicated that NF/BIN has a good potential as an ideal predictor of NF membrane separation behavior.

Keywords: Nanofiltration; Prediction system; User-friendly system; Binary salts

1. Introduction

Nanofiltration (NF) membranes, a relatively recent type of membranes, possess properties between ultrafiltration and reverse osmosis. The ionic transport mechanisms are, therefore, governed by both steric and charge effects [1]. This combined effect offers a value added to the membrane separation abilities, which covers almost all range of liquid–liquid separation system [2]. For all type of unit operation such as membrane separation system, having a good

*Corresponding author.

Presented at the Fifth Annual International Conference on "Challenges in Environmental Science & Engineering—CESE 2012" Melbourne, Australia, 9–13 September 2012

predictive tool is certainly vital in process performance prediction, hence process design and optimization.

The previous studies on NF membrane prediction show a rigorous improvement from time to time. Most researchers are concerned to update the existing predictive models to enhance the application of those models in order to optimize the separation prediction. However, the concern to develop a user-friendly prediction system applying an up to date and suitable software or simulator as an appropriate predictive tool is still inadequate.

The ability to predict the performance of NF membrane separations is very important in the design and operation of processes. Such prediction requires a characterization of key membrane parameters [3]. NF membranes are normally characterized by both the structural parameters such as pore radius and membrane thickness, and the electrical parameters, such as charge density.

The assessment of the significance of each ion transport mechanisms in the NF membrane; diffusion, electromigration, and convection are needed to comprehensively understand the ion transport behavior that would be very useful in improving the separation process. The literature shows lack of studies on the assessment of the ion transport mechanisms. In the preliminary stages, previous study successfully characterized and predicted the mechanisms for several commercial NF membranes and proved that each of the three modes of ion transport mechanism is significant [4]. The next stage, investigation on the transport mechanisms shows that each mode of the mechanisms strongly influenced by membrane charge density, permeate volume flux, pore radius, and effective membrane thickness to porosity ratio in determining the dominant modes at different operating conditions [5].

The purpose of this study is to develop a NF membrane separation prediction system for binary salts solutions. The graphical user interface (GUI) component of NF/BIN was designed to transform the conventional prediction task to be easier to perform and to graphically display the separation behavior including the assessment of percentage contribution of ion transport mechanisms; diffusion, electromigration, and convection, of the in-house-fabricated NF membranes. NF/BIN utilizes Donnan Steric Pore (DSP) model for membrane characterization and separation performance prediction.

1.1. Theory of the DSP model

Transport mechanisms of NF membrane were strongly influenced by both electrical (Donnan) and sieving (Steric) effects. Combination of these two effects allows NF membranes to be effective for a range of separation of mixtures of organic and salts. Three main ion transportation mechanisms involved, namely diffusion, electro-migration, and convection, which entirely governed in extended Nernst–Planck equation (Eq. (1)):

$$j_i = -D_{i,p}\frac{dc_i}{dx} - \frac{z_i c_i D_{i,p}}{RT}F\frac{d\varphi}{dx} + K_{i,c}c_i J \tag{1}$$

where j_i is flux of ion-i, $D_{i,p}$ is bulk diffusivity of ion-i, $K_{i,d}$ and $K_{i,c}$ are hindered factors for diffusion and convection, respectively. This equation served as main components in DSP model. In order to obtain an expression for rejection of the solute, Eq. (1) is integrated across the membrane thickness with solute concentrations at the upper ($x = 0$) and lower ($x = \Delta x$) surfaces expressed in terms of the external concentrations ($C_{i,x}$ and $C_{i,p)}$ using the equilibrium partition coefficient, Φ:

$$\Phi = \frac{c_{i,x=0}}{C_{i,x}} = \frac{c_{i,x=\Delta x}}{C_{i,p}} = \left(1 - \frac{r_s}{r_p}\right)^2 \tag{2}$$

Eqs. (1) and (2) can be integrated and combined to give the following expression for calculating real rejection:

$$R_{real} = 1 - \frac{K_{i,c}\Phi}{1 - \exp(-Pe_m)(1 - \Phi K_{i,c})} \tag{3}$$

where the Peclet number, Pe_m, is defined as follows:

$$Pe_m = \frac{K_{i,c}}{K_{i,d}}\frac{V\Delta x}{D_{i,\infty}A_k} \tag{4}$$

In the limiting case of the $Pe_m \to \infty$, the asymptotic rejection values (limiting rejection) will approach to $(1 - \Phi K_{i,c})$. Thus, $(1 - \Phi K_{i,c})$ represents a parameter of comparing the limiting rejection of solutes in membrane separation. The Hagen–Poiseuille equation relates the water flux to the applied pressure as well as r_p and $\Delta x/A_k$:

$$J_w = \frac{r_p^2 \Delta P}{8\mu(\Delta x/A_k)} \tag{5}$$

where J_w is flux of ion-i, r_p is membrane pore size, ΔP is operating pressure, $\Delta x/A_k$ is ratio of effective thickness to porosity, and μ is viscosity. Our previous study has shown that Donnan exclusion and Steric effects are significant in a small pore radii membrane, whereas steric hindrance is more prominent in relatively large pore radii membrane [6,7].

1.2. Ion transport mechanisms

In order to achieve the objective, the calculation of the contribution of each term in Eq. (1), the solution of the equation has been approximated with a one-step central difference method [8]. Thus:

$$\frac{dc_i}{dx} = \frac{c_i(x = \Delta x) - c_i(x = 0)}{\Delta x} \tag{18}$$

$$\frac{d\psi_m}{dx} = \frac{\psi_m(x = \Delta x) - \psi_m(x = 0)}{\Delta x} \tag{19}$$

where $x = 0$ indicates the membrane entrance and $x = \Delta x$ is the exit. The average concentration is defined as follows:

$$c_{i,avg} = \frac{c_i(x = \Delta x) - c_i(x = 0)}{2} \tag{20}$$

Using the above equations, the contribution of each transport mechanism can be calculated and represented in terms of the percentage of the total contribution.

Table 1
Main and supporting equations of DSP model

Donnan Steric Pore model	
Potential gradient:	
$\frac{d\varphi}{dx} = \frac{\sum_{i=1}^{n} \frac{z_i J_V}{d_{i,p}} (K_{i,c} C_i - C_{i,p})}{\frac{F}{RT} \sum_{i=1}^{n} z_i C_i}$	(6)
Concentration gradient:	
$\frac{dc_i}{dx} = \frac{J_V}{D_{i,p}} (K_{i,c} C_i - C_{i,p}) - \frac{z_i c_i}{RT} F \frac{d\varphi}{dx}$	(7)
Donnan equilibrium:	
$\frac{c_i}{c_{i,w}} = \phi \exp -\frac{z_i F}{RT} \Delta\varphi D$	(8)
where:	
$\phi = (1 - \lambda)$	(9)
Electroneutralities equations:	
Boundary layer:	
$\sum_{i=1}^{n} z_i C_{i,w} = 0$	(10)
Membrane:	
$\sum_{i=1}^{n} z_i C_{i,w} = -X_d$	(11)
Permeate:	
$\sum_{i=1}^{n} z_i C_{i,p} = 0$	(12)
Hindrance factors:	
$K_{i,d} = K^{-1}(\lambda, 0)$	(13)
$K_{i,c} = (2 - \phi) G(\lambda, 0)$	(14)
$D_{i,p} = K_{i,d} D_{i,\infty}$	(15)
$G(\lambda, 0) = 1.0 + 0.054\lambda - 0.988\lambda^2 + 0.441\lambda^3$	(16)
$K^{-1}(\lambda, 0) = 1.0 - 2.3\lambda + 1.154\lambda^2 + 0.224\lambda^3$	(17)

2. Methodology

The negatively charged membranes made of polyethersulfone/N-methylpyrolidone/water with different of polyethersulfone (PES) concentration (19, 21, and 23% w/w). Effective membrane area used in the experiment was 16.9 mm^2 and operating pressure of up to 10 bars. Glucose (MW = 180), maltose (MW = 342), and vitamin B12 (MW = 1,355) were chosen as neutral solutes, and sodium chloride 0.01 M was used as the model for charged solutes. The experimental data were then incorporated into the predictive tools to obtain full range of fluxes and rejection.

The DSP model takes into account the transport across the entire mentioned medium such as hydrodynamic parameters, drag forces, lag coefficient etc. [9] as described in Table 1. In this study, DSP models were utilized for binary solution (single salt solution), and the mathematical models were solved using MATLAB® m-file programming using modeling methodology as shown in Fig. 1.

The fabricated membranes were finally assessed its separation behavior in terms of percentage contribution of transport mechanisms; diffusion, electromigration, and convection and displayed on the designed GUI. The designing procedure of GUI is described in Fig. 2.

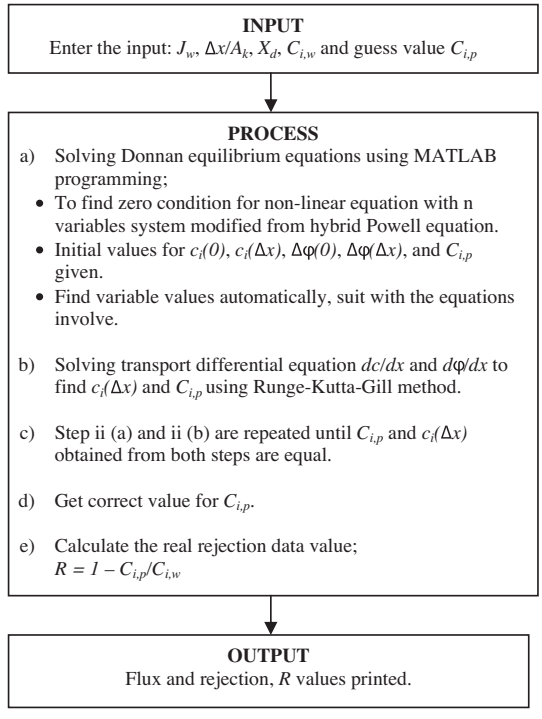

Fig. 1. Computer algorithm for modeling methodology.

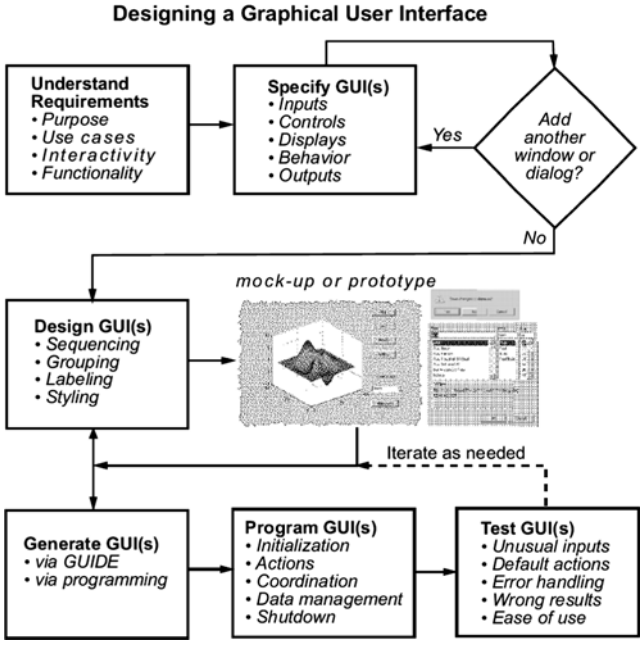

Fig. 2. Designing a GUI flowchart.

3. Results and discussion

3.1. Membrane characterization and performance evaluation

In all cases, the water flux was a linear function of the applied pressure, $J_v = P_m \Delta P$. The deviation from average values of permeability coefficient for all three samples of membrane were in the sequence of PES23 < PES21 < PES19. It is postulated that the pores of the membranes were quite nonuniform, and thus, the membrane possibly have wide pore size distribution.

For all membranes, the actual (real) rejection of uncharged solutes (glucose, maltose, and vitamin B12) was found to increase as the flux increased and approaching toward a limiting value, R_{lim}. Based on limiting rejection, r_p for each membrane was determined using Eqs. (2) and (3) and shown in the third column in Table 1. The r_p obtained for all membranes were synchronized with permeability coefficients, which confirmed the hydraulic stability of the fabricated membranes. The ratio of effective thickness over porosity, $\Delta x/A_k$ for each membrane was then determined from Eq. (5), as shown in the 5th column of Table 2. The value of $\Delta x/A_k$ for PES21 and PES23 is quite similar, even though their pore size and charged density are in the ratio of 1:2.

The structural parameters values of locally made PES membranes were within the range of reported values for commercially available membranes reported previously [10,11]. Table 2 shows the P_m, r_p, X_d, $\Delta x/A_k$, and ion chlorides rejection values obtained from DSP model.

Experiments were also carried out with NaCl at varying concentrations. In this study, DSP model was used to simulate experimental rejection data at a wide range of fluxes, in order to determine the dependency of the effective charge density (X_d) on the concentrations. The data input for this model, i.e. membrane structural parameters, was obtained from Table 2. Generally, the sequence of the rejection was as follows: PES23 > PES21 > PES19. Membrane PES23 showed highest chloride rejection, due to the combination of small pore size and large effective charge density (X_d) that caused the chloride ions to be easily rejected by the membranes [12]. For PES21 and PES19, even though the difference in r_p is rather small, the rejection of PES21 was almost double the PES19 rejection. This is postulated due to the higher X_d and $\Delta x/A_k$ inherent in PES21.

Fig. 3 shows the chloride rejection as a function of flux. Simulated lines were obtained from DSP model. The simulated and experimental data values lines show the feasibility of the developed NF/BIN to be used as a predictive tool of NF separation mechanisms. Consequently, it had been demonstrated that the fabricated membranes obeyed the DSP model which empirically represents the NF separation behavior.

3.2. User-friendly NF membrane prediction system (NF/BIN)

The first component of NF/BIN prediction system is m-file programming. This method was used to solve equations of mathematical model which describes NF membrane separation process in MATLAB®. Before applying any ordinary differential

Table 2
Structural parameter details of PES19, PES21, and PES23 membrane obtained from DSP model

ID	P_m (L/m^2 h bar)	r_p (nm)	X_d (molm^{-3})	$\Delta x/A_k$	Limiting Cl^- ions rejection (%)
PES19	2.58	1.36	22.8	11.8	24.5
PES21	1.98	1.11	45.8	25.4	35.0
PES23	0.72	0.76	150.8	24.5	79.2

equation (ODE) in MATLAB®, the mathematical model (equations) will be linearized and solved using MATLAB® command window, one of the elements in MATLAB® desktop. Function dissolve that symbolically was used to solve the ODE of DSP model that describes the ion transport processes through NF membranes.

A GUI is the link between software package and the user. In general, it is composed of a set of commands or menus, instruments, such as buttons, by means of which the user establishes a communication with the program [13]. The GUI minimizes the tasks of inputting data and displaying output data.

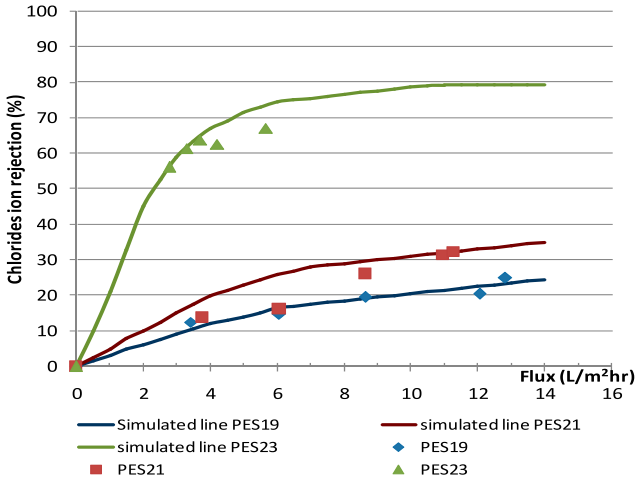

Fig. 3. Chloride ions rejection as a function of flux of PES membranes fabricated at various concentration.

"User-friendly" refers to anything that makes it easier for novices to use a computer. Menu-driven programs, for example, are considered more user-friendly than command-driven systems. GUIs are also considered user-friendly. NF/BIN can visualize the input/output parameter in one page screen. Compared to conventional prediction system, NF/BIN shortened the processing time of the simulation and the output directly visualized on the GUI after the program completely running [14]. By simply entering all the inputs and clicking the RUN button, the prediction task can be performed. Fig. 4 shows the designed GUI for the developed NF/BIN.

This kind of programming is often referred to as event-driven programming. In the designed GUI for NF/BIN, a button click is one such event. In event-driven programming, callback execution is asynchronous, that is, it is triggered by events external to the software. Callbacks, named for the fact that they "call back" to MATLAB® to ask it to do things [13,14]. Fig. 5 shows the call backs for push buttons for NF-BIN GUI component in m-file editor. In the case of MATLAB® GUIs, most events are user interactions with the GUI, but the GUI can respond to other kinds of events as well, for example, the creation of a file or connecting a device to the computer.

3.3. Analysis of ion transport mechanisms

As described in Section I (B), the contribution of each transport modes in the membrane can be calculated and represented in terms of percentage of the total contribution using Eqs. (18–20). The analysis has

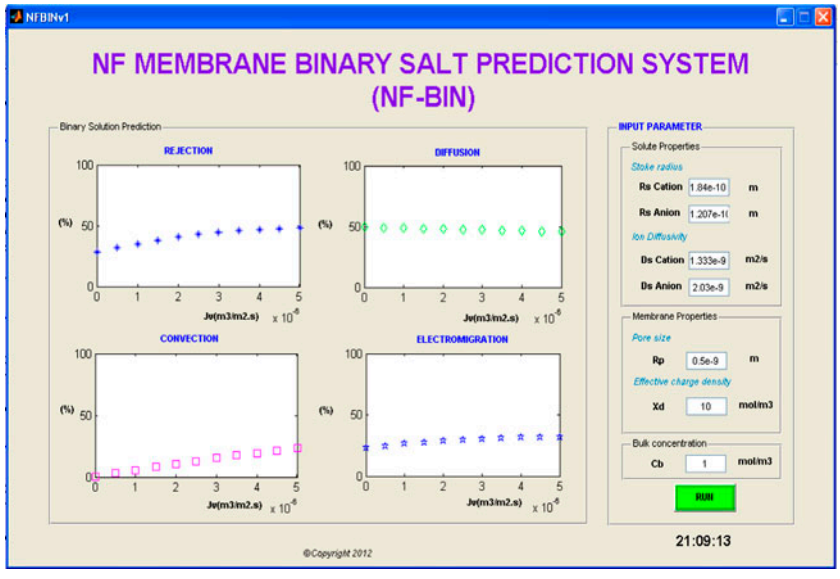

Fig. 4. GUI component of NF-BIN.

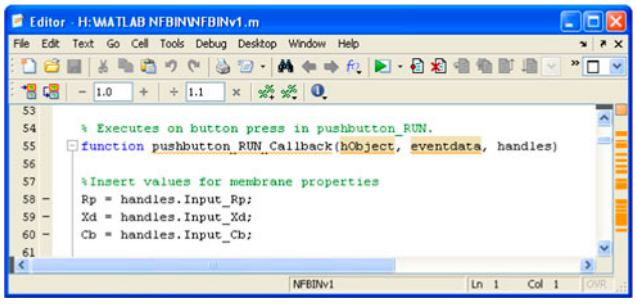

Fig. 5. Call back m-file editor for push buttons.

Table 3
Assessment of ion transport mechanisms percentage contribution for the PES membranes fabricated at various concentration at the limiting rejection

ID	Limiting Cl^- ions rejection	Diffusion (%)	Electromigration (%)	Convection (%)
PES19	24.5	66	18	16
PES21	35.0	65	21	13
PES23	79.2	60	28	12

been carried out for NaCl, and the solute flux (j_i) for Cl^- ion has been calculated in total and in its components. The data are represented as a function of flux. The analysis has been carried for the fabricated PES membrane using the data obtained in the characterization analysis. Table 3 shows the analysis of three fabricated PES membranes.

Inside the membrane, the diffusion, convection, and electromigration transport components of Cl^- ions will act toward the permeate side but for Na^+ ions only the diffusion and convection transport components are toward the permeate with the electromigration in the opposite direction [8]. All three transport mechanisms are seen to be significant. Elecromigration and convection show lower percentage contribution while convection exhibits the lowest measurement.

Diffusion is likely to be the dominant mechanism involved for all the locally fabricated NF membranes with different structural parameters that strongly influenced the separation behavior. Transport is mainly governed by diffusion, when the membrane is strongly charged, particularly at low permeate volume flux and effective membrane thickness to porosity ratio, $\Delta x/A_k$ [5]. Consequently, in order to optimize the separation process for engineering purposes, the diffusion should be further promoted by modifying the parameters governed in the diffusion mode to obtain the higher and optimum possible values.

4. Conclusion

The developed NF/BIN as a NF membrane separation predictive tool based on DSP model is very useful in predicting and explaining the behavior as well as in determining the structural parameters of locally developed NF membranes. Prediction of ion transport mechanisms is crucial to further enhance separation performance in NF processes. This proved that the developed NF/BIN can provide a platform for ion transport mechanism prediction in the conjunction to achieve process optimization.

Symbols

c_i — concentration in membrane (mol m^{-3})
$C_{i,b}$ — concentration in the bulk solution (mol m^{-3})
$C_{i,p}$ — concentration in permeate (mol m^{-3})
$C_{i,w}$ — concentration at the membrane wall (mol m^{-3})
$D_{i,p}$ — hindered diffusivity (m^2 s^{-1})
$D_{i,\infty}$ — bulk diffusivity (m^2 s^{-1})
F — Faraday constant (C mol^{-1})
G — the hydrodynamic lag coefficient
K^{-1} — the hydrodynamic enhanced drag coefficient
j_i — ion flux (based on membrane area) (mol m^{-2} s^{-1})
$K_{i,c}$ — hindrance factor for convection
$K_{i,d}$ — hindrance factor for diffusion
P_m — membrane permeability (m^3 s^{-1} m^{-2} bar^{-1})
r_p — effective pore radius (m)
R — gas constant (J mol^{-1} K^{-1})
R_{real} — real rejection of the solute
T — absolute temperature (K)
x — distance normal to membrane (m)
Δx — effective membrane thickness (m)
X_d — effective membrane charge (mol m^{-3})
z_i — valence of ion
δ — thickness of film layer (m)
ΔP — applied pressure drop (bar)
Φ — coefficient as defined by Eq. (9)
$\Delta\psi$ — potential difference (V)

References

[1] A.W. Mohammad, N.a. Ali, Understanding the steric and charge contributions in NF membranes using increasing MWCO polyamide membranes, Desalination 147(1–3) (2002) 205–212.
[2] A.W. Mohammad, L.Y. Pei, A.H. Khadum, Characterization and identification of rejection mechanisms in nanofiltration membranes using extended Nernst–Planck model, Clean Technol. Environ. Policy 4 (2002) 151–156.
[3] A.W. Mohammad, M.S. Takriff, Predicting flux and rejection of multicomponent salts mixture in nanofiltration membrane, Desalination 157 (2003) 105–111.
[4] W.R. Bowen, J.S. Welfoot, Predictive modelling of nanofiltration: Membrane specification and process optimization, Desalination 147(1–3) (2002) 197–203.

[5] A. Szymczyk, C. Labbez, P. Fievet, A. Vidonne, A. Foissy, J. Pagetti, Contribution of convection, diffusion and migration to electrolyte transport through nanofiltration membranes, Adv. Colloid Interface Sci. 103 (2003) 77–94.
[6] N.a. Ali, N.S. Suhaimi, Performance evaluation of locally fabricated asymmetric nanofiltration membrane for batik industry effluent, Adv. Colloid Interface Sci. 5 (Special Issue for Environment) (2009) 46–52.
[7] N.a. Ali, A.W. Mohammad, A.L. Ahmad, Use of nanofiltration predictive model for membrane selection and system cost assessment, Sep. Purif. Technol. 41 (2005) 29–37.
[8] W.R. Bowen, A.W. Mohammad, Characterization and prediction of nanofiltration membrane performance—A general assessment, Sep. Purif. Technol. 76 (1998) 885–893.
[9] W.R. Bowen, H. Mukhtar, Characterisation and prediction of separation performance of nanofiltration membranes, J. Membr. Sci. 112(2) (1996) 263–274.
[10] W.R. Bowen, A.W. Mohammad, N. Hilal, Characterisation of nanofiltration membranes for predictive purposes: use of salts, uncharged solutes and atomic force microscopy, J. Membr. Sci. 126(1) (1997) 91–105.
[11] N.S. Kotrappanavar, A.A. Hussain, M.E.E. Abashar, I.S. Al-Mutaz, T.M. Aminabhavi, M.N. Nadagouda, Prediction of physical properties of nanofiltration membranes for neutral and charged solutes, Desalination 280(1–3) (2011) 174–182.
[12] A.W. Mohammad, N. Hilal, H. A-Zoubi, N.A. Darwish, W.R. Bowen, Prediction of permeate fluxes and rejections of highly concentrated salts in nanofiltration membranes, J. Membr. Sci. 289(1–2) (2007) 40–50.
[13] D. Baez-Lopez, MATLAB® with applications to engineering, physics and finance, CRC Press, Boca Raton, 2010.
[14] S.J. Chapman, MATLAB® Programming for Engineers and Scientists, 3rd ed., Thomson Canada Ltd, Canada, 2005.